SAND2013-9519C

Label-Free Plasmonic Immunosensing for Plasmodium in Whole Blood

Sang-Yeon Cho[1,*], Jayson L. Briscoe[1], Immo A. Hansen[2], Jesse K. Smith[2], Yoomi Chang[3], and Igal Brener[4,5]
[1]Klipsch School of Electrical and Computer Engineering, New Mexico State University, Las Cruces, NM, USA
[2]Department of Biology and Institute of Applied Biosciences, New Mexico State University, Las Cruces, NM, USA
[3]Department of Chemistry and Biochemistry, New Mexico State University, Las Cruces, NM, USA
[4]Sandia National Laboratories, Albuquerque, NM, USA
[5]Center for Integrated Nanotechnologies, Albuquerque, NM, USA
Email: *sangycho@nmsu.edu

***Abstract*— We present the first experimental demonstration of label-free malaria pathogen detection in whole blood lysate using plasmon nanostructures. Previous studies on plasmonic biosensing have measured antibody-antigen binding, protein-protein interactions, and detection of bacteria. However, unlike our sensor, many of these works rely on complex optical setups to excite surface plasmon waves. The demonstrated plasmon sensor is a compact, highly sensitive, cost effective, selective diagnostic tool for many portable biosensing applications such as point-of-care diagnostics. To achieve malaria pathogen detection, we utilized a highly site-directed and stable antibody immobilization process on the nanostructure's surface. The measured refractive index sensitivity of the nanostructured sensor is 378 nm/RIU in the visible range. Introduction**

A new study estimates that 1.2 million people died in 2010 from malaria [1]. Early detection and treatment reduces disease transmission and quantitative detection of malaria pathogens, sporozoans of the genus Plasmodium, is crucial to avoid improper diagnoses. A number of diagnostic approaches for the detection of Plasmodium in human blood samples have been developed including microscopic evaluation of Giemsa-stained blood smears [2], enzyme-linked immunosorbent assay (ELISA) [3], immunochromatography [4], polymerase chain reaction (PCR) assay [5], and a large variety of rapid detection methods based on lateral flow or dipstick assays [6]. Visual inspection using an optical microscope has been a standard method for detecting the presence of the pathogens. This approach requires trained personnel and laboratory equipment to prepare specimens. ELISA requires multiple preparation steps to label antibodies with particles that can provide detectable signals, such as fluorescence. The signal strength of immunochromatography is typically weak. In addition, this approach is rarely quantitative, which can lead to an improper diagnosis. In PCR, highly trained personnel and laboratory equipment are needed to prepare specimens, thus it is time-consuming and expensive.

In this paper, we present an experimental demonstration of sensitive and selective detection of Plasmodium parasites in a whole blood lysate using diffraction-assisted extraordinary optical transmission (EOT) through periodically coupled metallic nanostructures. To our knowledge, this is the first experimental demonstration of Plasmodium detection in blood samples by directly probing antibody-antigen interactions with EOT. The demonstrated biosensor is a compact, highly sensitive, selective diagnostic tool for portable biosensing applications.

This research is funded by the Bill and Melinda Gates Foundation through Grand Challenges Explorations.

I. Sensor Design

A. Background: Plasmonic Sensing

Surface plasmon resonance (SPR) offers extremely high surface sensitivity and has been widely used in various detection applications such as the interaction of nucleic acids with small molecules [7], biomolecular interactions in blood samples [8], and antibody-antigen interactions [9]. An SPR sensor detects changes in the excitation condition of a surface plasmon wave (SP) on a metal-dielectric interface. In conventional SPR sensors, additional couplers, such as a prism, are required to provide an extra wave-vector component to incident light [10], making the sensor bulky and vulnerable to mechanical vibration noises. A nanoparticle based sensor utilizes localized surface plasmon resonance (LSPR) to probe analytes. The nanoparticle sensor measures changes in the extinction spectrum of LSPR. However, the extinction spectrum of an LSPR-based nanoparticle sensor can be affected by many factors including shape, size, and its composition [11], resulting in reduced sensitivity. Several lithographically patterned plasmon sensors have been reported [12]-[14]. Unlike nanoparticle based sensors, the spectral response of a patterned plasmon sensor can be precisely controlled and engineered [15]-[19]. Nanostructured plasmon sensors, such as nanohole arrays, have been widely used in a number of sensing applications including measurement of protein-protein interactions [20], detection of bacteria [21], tumor markers [22], and antibody-antigen interactions [23], [24]. Enhanced refractive index sensitivity has been demonstrated using the resonant surface modes in a defect-assisted plasmonic crystal [25].

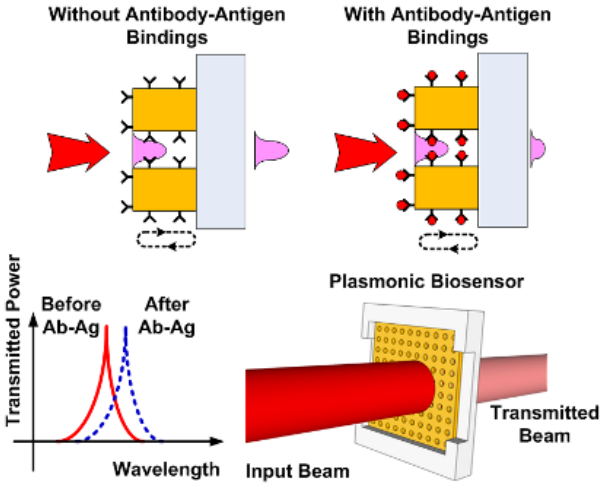

Figure 1. Detection mechanism of the plasmon biosensor. The refractive index change induced by the antibody-antigen interaction on the surface of the plasmon sensor is detected by monitoring the transmission spectra through nanostructures.

The plasmon biosensor reported here uses enhanced optical transmission through periodic nanostructures to probe refractive index change due to antibody-antigen interactions. The plasmon sensor consists of an array of periodic nanoholes in a metal film, a layer of crosslinkers, and a bio-transducer. The bio-transducer, a layer of immobilized antibody, responds to target pathogens, creating refractive index perturbation on the surface. The induced index perturbation alters the dispersion relation, the ω–β diagram, of the SP wave on the sensor. Fig. 1 shows a schematic drawing of the biosensor. The patterned nanostructures convert the incoming light into the surface waves on the sensor. Unlike photons, the excited surface waves can significantly enhance the transmission of incoming wave through the subwavelength holes. This SP wave is extremely sensitive to changes in the refractive index of the surrounding medium. By monitoring the transmission spectrum of the sensor, induced refractive index perturbation can be accurately measured.

The refractive index perturbation of the biosensor can be measured by wavelength or intensity interrogation. Wavelength interrogation is achieved by monitoring the transmission spectrum of the plasmon sensor using a spectrometer and a broadband optical source. Resonant peaks due to EOT in the transmission spectrum can be used to measure the changes in the refractive index from antibody-antigen interactions. For intensity interrogation, the transmitted intensity of the sensor at a fixed wavelength is monitored using a calibrated photodetector.

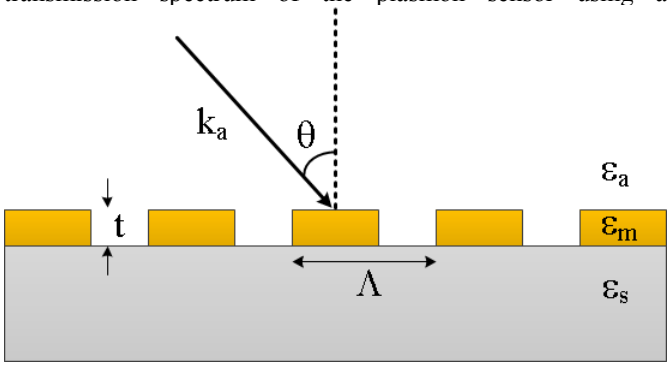

Figure 2. Exictation of SP waves using a periodic nanostructure.

B. Plasmon Sensor Design and Fabrication

Fig. 2 depicts the excitation mechanism of the plasmon sensor. When an incident beam interacts with a periodic nanostructure, multiple diffracted waves are excited. The excitation of the SP waves can be described by

$$\beta = k_a \sin(\theta) \pm m K_G \qquad (1)$$

where β is the wave vector of the excited plasmon wave, k_a is the wave vector of the incident wave, θ is the angle of incidence, m is an integer, and $K_G = 2\pi/\Lambda$ is the reciprocal vector of the nanostructure. β in (1) can be obtained by solving the characteristic equation of a three-layer guiding structure [26],

$$\exp(2t\,k_m) = \frac{(k_m\varepsilon_a - k_a\varepsilon_m)(k_m\varepsilon_s - k_s\varepsilon_m)}{(k_m\varepsilon_a + k_a\varepsilon_m)(k_m\varepsilon_s + k_s\varepsilon_m)} \qquad (2)$$

Where $k_i^2 = \beta^2 - k_0^2\varepsilon_i$, $i = a, m, s,$ and k_0 is the wave vector in free space. Excited SP waves play a vital role in enhanced optical transmission [27],[28], serving as a probe for antibody-antigen interaction. In addition to the role of SP waves, several phenomena contribute to improved optical transmission through the nanostructure [29]-[31]. Excitation of the SP wave is detected as a peak in the transmission spectrum.

The enhanced optical transmission of the plasmon sensor is analyzed by performing electromagnetic simulations of the nanohole array using COMSOL Multiphysics™. For simulation, periodic boundary conditions are used to address repeated nanoholes. To avoid undesired numerical reflections, boundaries of the computational window are terminated by perfectly matched layers. A TM-polarized plane wave is used as an optical excitation. The modified Lorentz-Drude model [32] is used to include the dispersion characteristics of gold. The dimensions of the sensor are designed to achieve EOT around λ=725 nm.

The sensors were fabricated by a focused-ion-beam system. A 100 nm-thick Au layer was deposited on a microscope slide. The nanoholes were 200 nm in diameter with 300 nm separation between the adjacent holes. For experimental characterization, the output spectrum of the sensor was measured by using a quartz-tungsten-halogen lamp and a fiber-coupled spectrometer. This measurement was performed before applying the bio-transducer layer. The calculated and measured transmission spectra of the biosensor in water at surface normal excitation are presented in Fig. 3. The inset of Fig. 3 shows a scanning electron microscope (SEM) image of the fabricated sensor.

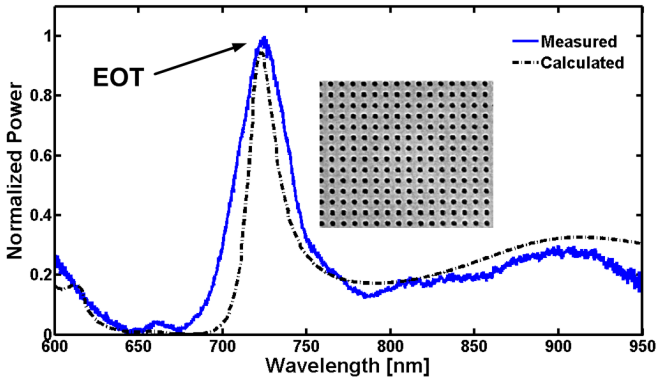

Figure 3. Calculated (dotted curve) and measured (solid curve) transmission spectra of the fabricated sensor in DI water. A quartz-tungsten-halogen lamp was used for a broadband optical source.

II. Experimental Characterization

The refractive index sensitivity of the fabricated sensor was measured using different concentrations of glucose in deionized (DI) water. The variation of refractive index with concentration of glucose in DI water is well known [33]. The spectral response of the fabricated plasmon sensor was measured by applying different glucose solutions. In each measurement, the sensor surface was thoroughly rinsed with DI water. The spectral response of the sensor in water serves as the baseline for this experiment. Fig. 4 shows the measured wavelength shifts of the peak for five different glucose concentrations in DI water. As shown in the figure, the spectral responses of the sensor are fully restored after rinsing the surface of the sensor with DI water. Using simple linear regression, the estimated index sensitivity of the peak is 378 nm per refractive index unit (RIU).

The transmission spectra of the biosensor were measured during the antibody immobilization process. The characterization procedure of the fabricated sensor is as follows: the output spectrum of the sensor in DI water was measured before applying the surface chemistry to immobilize antibodies. Protein A was covalently attached to the gold surface using dithiobis succinimidyl protioate (DSP) as a linker. Monoclonal antibodies (#14c, Flow Incorporated, OR) against Plasmodium lactate dehydrogenase, were immobilized through strong binding with Protein A. After immobilizing antibodies on the surface, we measured the output transmission spectrum which serves as the baseline of the immunoassay. Blood samples from a malaria-infected chicken were then lysed and introduced on the surface of the sensor. An optical microscopic parasitemia inspection showed that 10% of the red blood cells were infected with Plasmodium parasites. The output spectrum of the sensor was measured again. The presence of various biomolecules in the blood sample introduced a redshift in the output response. Finally, the sensor surface was rinsed with DI water and the output spectrum was measured. A blueshift is observed in the output spectrum. The measured blueshift is caused by removing unwanted biomolecules from the sensor surface, leaving only the antigen-antibody pairs on the sensor. The observed blueshift confirms that undesired artifacts in the measurement

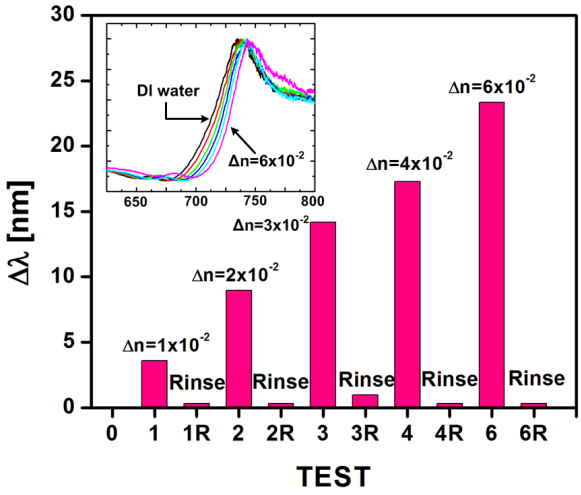

Figure 4. Measured wavelength shifts of the resonant peak for different glucose concentrations. The sensor was rinsed with DI water and measured to ensure a reset of the sensing surface. Inset: Measured tranmission spectra of the sensor for varying glucose concentrations.

due to fouling can be significantly reduced by rinsing the surface of the sensor with DI water.

Fig. 5 shows the transmitted intensity of the sensor monitored at a fixed wavelength within the enhanced transmission band at each step. The spectral band is shown in the inset of Fig. 4. A noticeable change in transmitted intensity between the antibody immobilization step and the final rinse was observed. This change in intensity indicates a refractive index change at the sensor's surface due to antibody-antigen interaction. To confirm our results were from antibody-antigen interactions, both a positive and negative control test were performed. Whole blood from an uninfected chicken was lysed and introduced onto the sensor. The transmission spectrum was measured, representing the negative control, and the surface was thoroughly rinsed. Next, whole blood from a malaria infected chicken was lysed and introduced onto the biosensor. A noticeable red-shift of the transmission spectrum is observed for the positive control as compared to the negative control. The control experiments confirm the selectivity of the sensor to the target malaria parasites.

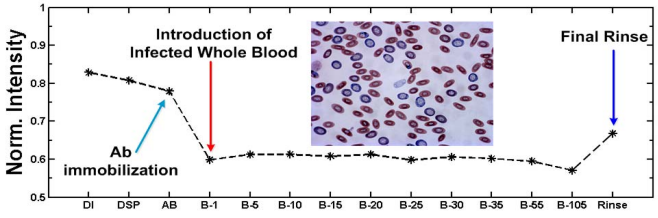

Figure 5. Intensity monitoring of the transmission spectrum was performed after each process step represented as follows: "DI": deionized water, "DSP": introduction of the cross-linker DSP on the sensor, "AB": immobilization of monoclonal antibodies, "B-X": X number of minutes after whole blood lysate was introduced, "Rinse": rinsed the sensor with DI water six times. A noticeable change in transmitted intensity is observed when comparing Ab immobilization and final rinse indicating antibody-antigen interaction. Inset-Results from an optical microscopic parasitemia inspection. Approximately 10% of red blood cells were infected with Plasmodium parasites.

ACKNOWLEDGMENT

This research is funded by a grant from the Bill & Melinda Gates Foundation through the Grand Challenges Exploration Initiative. This work was performed in part at the US Department of Energy, Center for Integrated Nanotechnologies, Sandia National Laboratories (Contract DE-AC04-94AL85000). The authors would like to thank Dr. Michael Makler of Flow Inc. for providing antibodies used in this study.

REFERENCES

[1] C.Y. Murray, L.C. Rosenfeld, S.S. Lim, K.G. Andrews, K.J. Foreman, D. Harrington, N. Fullman, M. Naghavi, R. Lozano, and A.D. Lopez, Global malaria mortality between 1980 and 2010: a systematic analysis. Lancet. 379, 2012, pp. 413-431.

[2] B. K. Wilson, M. R. Behrend, M. P. Horning, and M. C. Hegg, Detection of malarial byproduct hemozoin utilizing its unique scattering properties, Opt. Express 19, 2011, pp. 12190-12196.

[3] P. Yager, G. J. Domingo, and J. Gerdes, Point-of-care diagnostics for global health, Annu. Rev. Biomed. Eng. 10, 2008, pp. 107-144.

[4] L. Bissonnette, M. G. Bergeron. Diagnosing infections--current and anticipated technologies for point-of-care diagnostics and home-based testing, Clin. Microbiol. Infect. 16, 2010, pp. 1044-1053.

[5] C. Bass, D. Nikou, A. M. Blagborough, J. Vontas, R. E. Sinden, M. S. Williamson, and L. M. Field, PCR-based detection of Plasmodium in Anopheles mosquitoes: a comparison of a new high-throughput assay with existing methods, Malaria Journal, 2008, 7:177.

[6] B. S. Kakkilaya, Rapid Diagnosis of Malaria, Lab Medicine 34, 2003, pp. 602-608.

[7] Y. Liu, W. D. Wilson, Quantitative analysis of small molecule-nucleic acid interactions with a biosensor surface and surface plasmon resonance detection, Methods Mol. Biol. 613, 2010, pp. 1-23.

[8] T. Springer, M. Piliarik, and J. Homola, Real-time monitoring of biomolecular interactions in blood plasma using a surface plasmon resonance biosensor, Anal. Bioanal. Chem. 398, 2010, pp. 1955-1961.

[9] K. M. Mayer, S. Lee, H. Liao, B. C. Rostro, A. Fuentes, P. T. Scully, C. L. Nehl and J. H. Hafner, A Label-Free Immunoassay Based Upon Localized Surface Plasmon Resonance of Gold Nanorods, ACS Nano 2, 2008, pp. 687–692.

[10] H. Raether, Surface Plasmons on Smooth and Rough Surfaces and on Gratings (Springer-Verlag, 1988).

[11] J. Kottmann, O. Martin, D. Smith, and S. Schultz, Spectral response of plasmon resonant nanoparticles with a non-regular shape, Opt. Express 6, 2000, pp. 213-219.

[12] J. L. Briscoe and S.-Y. Cho, A periodically coupled plasmon nanostructure for refractive index sensing, Opt. Express 19, 2011, pp. 8815-8820.

[13] S. Roh, T. Chung and B. Lee, Overview of the Characteristics of Micro- and Nano-Structured Surface Plasmon Resonance Sensors, Sensors 11, 2011, pp. 1565-1588.

[14] J. N. Anker, W. P. Hall, O. Lyandres, N. C. Shah, J. Zhao, and R. P. Van Duyne, Biosensing with plasmonic nanosensors, Nature Materials 7, 2008, pp. 442 - 453.

[15] J. L. Briscoe and S.-Y. Cho, Hybrid plasmonic resonance for enhanced refractive index sensing, Electron. Lett., 47, 2011, pp. 1294-1295.

[16] D. A. Schultz, J. J. Mock, S. Schultz, D. R. Smith, Single-Target Molecule Detection with Nonbleaching Multicolor Optical Immunolabels, Proc. Natl. Acad. Sci. 97, 2000, pp. 996–1001.

[17] A. Lesuffleur, H. Im, N. C. Lindquist, and S.-H. Oh, Periodic nanohole arrays with shape-enhanced plasmon resonance as real-time biosensors, Appl. Phys. Lett. 90, 2007, pp. 243110.

[18] F. Eftekhari, R. Gordon, J. Ferreira, A. G. Brolo, and D. Sinton, Polarization-dependent sensing of a self-assembled monolayer using biaxial nanohole arrays, Appl. Phys. Lett. 92, 2008, pp. 253103.

[19] E. M. Hicks, X. Zhang, S. Zou, O. Lyandres, K. G. Spears, G. C. Schatz, and R. P. Van Duyne, Plasmonic Properties of Film over Nanowell Surfaces Fabricated by Nanosphere Lithography, J. Phys. Chem. B 109, 2005, pp. 22351-22358.

[20] L. Feuz, P. Jonsson, M. P. Jonsson and F. Hoo□k, Improving the Limit of Detection of Nanoscale Sensors by Directed Binding to High-Sensitivity Areas, ACS Nano 4, 2010, pp. 2167–2177.

[21] S. Chen, M. Svedendahl, M. Kall, L. Gunnarsson, and A. Dmitriev, Ultrahigh sensitivity made simple: nanoplasmonic label-free biosensing with an extremely low limit-of-detection for bacterial and cancer diagnostics, Nanotechnology 20,2009, 434015.

[22] D. Gao, W. Chen, A. Mulchandani, J. S. Schultz, Detection of tumor markers based on extinction spectra of visible light passing through gold nanoholes, Appl. Phys. Lett. 90, 2007, 073901.

[23] J. Ji, J. O'Connell, D. Carter, and D. Larson, High throughput nanohole array based system to monitor multiple binding events in real time, Anal. Chem 80, 2008, pp. 2491-2498.

[24] T. Endo, K. Kerman, N. Nagatani, H. M. Hiepa, D.-K. Kim, Y. Yonezawa, K. Nakano, and E. Tamiya, Multiple Label-Free Detection of Antigen−Antibody Reaction Using Localized Surface Plasmon Resonance-Based Core−Shell Structured Nanoparticle Layer Nanochip, Anal. Chem. 78, 2006, pp. 6465–6475.

[25] J. L. Briscoe, S.-Y. Cho, and I. Brener, "Defect-assisted plasmonic crystal sensor," Opt. Lett. 38, 2013, pp. 2569-2571.

[26] S. A. Maier, Plasmonics: Fundamentals and Applications, (Springer, 2007).

[27] H. F. Ghaemi, T. Thio, and D. E. Grupp, T. W. Ebbesen, and H. J. Lezec, Surface plasmons enhance optical transmission through subwavelength holes, Phys. Rev. B 58, 1998, pp. 6779- 6782.

[28] S. A. Darmanyan and A.V. Zayats, Light tunneling via resonant surface plasmon polariton states and the enhanced transmission of periodically nanostructured metal films: An analytical study, Phys. Rev. B 67, 2003, 035424.

[29] S.-H. Chang, S. Gray, and G. Schatz, Surface plasmon generation and light transmission by isolated nanoholes and arrays of nanoholes in thin metal films, Opt. Express 13, 2005, pp. 3150-3165.

[30] C. Genet, M.P. van Exter, and J.P. Woerdman, Fano-type interpretation of red shifts and red tails in hole array transmission spectra, Opt. Commun. 225, 2003, pp. 331-336.

[31] J. M. McMahon, J. Henzie, T. W. Odom, G. C. Schatz, and S. K. Gray, Tailoring the sensing capabilities of nanohole arrays in gold films with Rayleigh anomaly-surface plasmon polaritons, Opt. Express 15 (2007) 18119-18129.

[32] A. Rakić, A.B. Djurišić, J. Elazar, and M.L. Majewski, Optical properties of metallic films for vertical-cavity optoelectronic devices, App. Opt. 37 (1998) 5271-5283.

[33] Y.-L. Yen, C. C. Wang, M.-J. Jang, C.-H. Chen, S.-M. Tzeng, Y.-P. Lin, K. S. Chen, Real-time measurement of glucose concentration using position sensing detector, presented at the 3rd IEEE International Conference on Nano/Micro Engineered and Molecular Systems, China, 6-9 Jan. 2008.